VLSI IMPLEMENTED ML JOINT CARRIER PHASE AND TIMING OFFSETS ESTIMATOR FOR QPSK/OQPSK BURST MODEMS

Yimin Jiang*, Farhad B. Verahrami*, Wen-Chun Ting*, Robert L. Richmond*, John S. Baras+

* Hughes Network Systems, Inc, 11717 Exploration Lane
Germantown, MD 20876, E-mail: yjiang@hns.com
+ Institute for Systems Research, University of Maryland
College Park, MD 20742, E-mail: baras@isr.umd.edu

ABSTRACT

A high performance ASIC supporting multiple modulation, error correction, and frame formats is under development at Hughes Network Systems, Inc. Powerful and generic data-aided (DA) estimators are needed to accommodate operation in the required modes. In this paper, a simplified DA maximum likelihood (ML) joint estimator for carrier phase and symbol timing offset for QPSK/OQPSK burst modems and a sample systolic VLSI implementation for the estimator are presented. Furthermore, the Cramer-Rao lower bound (CRLB) for DA case is investigated. The performance of the estimator is shown through simulation to meet the CRLB even at low signal-to-noise ratios (SNR). Compared with theoretical solutions, the proposed estimator is less computationally intensive and is therefore easier to implement using current VLSI technology.

1. INTRODUCTION

A high performance ASIC supporting Hughes Network System's Universal Modem product line is under development. This ASIC will support a variety of bit rates, modulations (BPSK, QPSK, 8PSK, OQPSK), forward error correction, and frame formats. The ASIC will use several burst parameter estimation algorithms, these algorithms are generic enough to be applicable in all of the various modes and can be readily implemented in hardware.

An expression for the DA ML joint carrier phase and timing offsets estimator in time-domain was derived in [1] (p.296). Implementing the estimator is however, somewhat hardware intensive. Based on the work in [1], a new algorithm has been derived that can be also extended to the OQPSK case. This algorithm is relatively simple and is suitable for systolic VLSI implementation. The performance lower bound for ML estimation is the CRLB. An expression for the CRLB for timing recovery in the non-DA case is given in [3]. Jiang has derived an expression for an ML joint phase and timing offset estimator, and the CRLB for the DA timing recovery case based on a frequency domain approach in [2]. In the DA case, the CRLB_{DA}
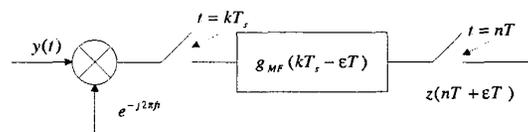

Figure 1: Matched Filter of Optimal Receiver

(for DA case) which provides insight on data pattern selection for faster timing recovery is investigated further in this paper.

In section 2 a derivation of the estimation algorithm is presented. Section 3 presents an efficient VLSI implementation of the estimator. In the last section the CRLB for the non-DA case and the CRLB_{DA} are investigated, and the performance of the new estimator is shown through computer simulation and compared with CRLB_{DA}.

2. ESTIMATION ALGORITHM

The baseband received signal is modeled as:

$$y(t) = \sqrt{E_s} \sum_{n=0}^{N-1} [(a_{In}g(t - nT) + ja_{Qn}g(t - nT - \tau T)) \exp[j(2\pi ft + \theta)]] + n(t) \tag{1}$$

where $g(t) = g_T(t) \otimes c(t) \otimes f(t)$, $g_T(t)$ is the transmitter shaping function, $c(t)$ is the channel response, $f(t)$ is the prefilter, $n(t)$ is the additive white Gaussian noise (AWGN) with two-sided power spectral density $N_0/2$, and $a_n \equiv a_{In} + ja_{Qn}$ is the data symbol from complex plane ($a_n = \sqrt{2}/2(\pm 1 \pm j)$ for QPSK/OQPSK signaling). T is the symbol interval, f is the carrier frequency offset, and τ is the delay factor that is 0 for QPSK and 0.5 for OQPSK. The estimation algorithm for the QPSK case is as follows. The matched filter for an optimal receiver can be modeled as [1] shown in Figure 1. $y(t)$ is down converted by carrier frequency offset estimate $\hat{f}$, and then sampled at rate of $1/T_s$, typically $T = LT_s$, with L an integer. The sampled signal is filtered by a matched shaping filter with

response $g(-t)$ and timing offset εT. The output is then decimated down to a rate of $1/T$ to obtain a one sample per symbol signal $z(nT + \varepsilon T)$. The demodulator corrects the phase offset θ and timing offset ε of $z(nT + \varepsilon T)$ prior to making symbol decisions and recovering the transmitted symbol $\hat{a}_n$. $z(nT + \varepsilon T)$ is given by:

$$z(nT + \varepsilon T) = \sum_{k=-\infty}^{\infty} y(kT_s)e^{-j(2\pi f k T_s)}g_{MF}(nT + \varepsilon T - kT_s) \qquad (2)$$

Assuming zero frequency offset estimation error, there are K ($K = LN$) observations of $z(kT_s + \varepsilon T)$ ($k = 0, \cdots, K - 1$) available for estimating ε and θ, $\varepsilon \in [-0.5, 0.5)$. According to the work done in [1], the maximization object function of ML joint phase and timing offsets estimation in AWGN channel is

$$L(\underline{a}, \varepsilon, \theta) = C \exp \left\{ -\text{Re}\left[\sum_{n=0}^{N-1} a_n^* z(nT + \varepsilon T)e^{-j\theta} \right] \right\} \qquad (3)$$

where C is a positive constant and $\underline{a} = [a_0, \cdots, a_{N-1}]$ which is the data pattern and is known to the estimator. Let us define $\mu(\varepsilon)$ as:

$$\mu(\varepsilon) = \sum_{n=0}^{N-1} a_n^* z(nT + \varepsilon T) \qquad (4)$$

The ML joint phase and timing estimator is given by [1]:

$$\hat{\varepsilon} = \arg \max_\varepsilon |\mu(\varepsilon)| \qquad (5)$$

$$\hat{\theta} = \arg[\mu(\hat{\varepsilon})] \qquad (6)$$

According to the Equivalence Theorem [1], and assuming that $c(t)$ and $f(t)$ are all-pass filters, $z(nT + \varepsilon T)$ is equivalent to the following:

$$z(nT + \varepsilon T) = \sum_{k=0}^{N-1} a_k r(nT + \varepsilon T - kT)e^{-j\theta} + N_n \qquad (7)$$

$$\text{where } r(t) = g_T(t) \otimes g_T(-t)$$

$$= \frac{sin(\pi t/T)}{\pi t/T} \frac{cos(\alpha \pi t/T)}{1 - 4\alpha^2 t^2/T^2}$$

The above expression also assumes that raised cosine shaping is adopted with α denoting the rolloff factor. N_n is the sampled version of $n(t)$, Gaussian noise, after being filtered by $g_{MF}(t)$.

Arriving at a solution to eq. (5) is a difficult task and the resulting hardware structure presented in [1] is quite complicated. It is well known that a quadratic form can be used to approximate the central segment of a convex function around its peak. The expression for $\mu(\varepsilon)$ can be approximated by a quadratic equation as shown below. If $\varepsilon \to 0$, the inter-symbol-interference (ISI) and noise N_n can be ignored and we can simplify $|\mu(\varepsilon)|$ as

$$|\mu(\varepsilon)| \approx E_s \sum_{n=0}^{N-1} |a_n|^2 r(\varepsilon T) = N E_s r(\varepsilon T) \qquad (8)$$
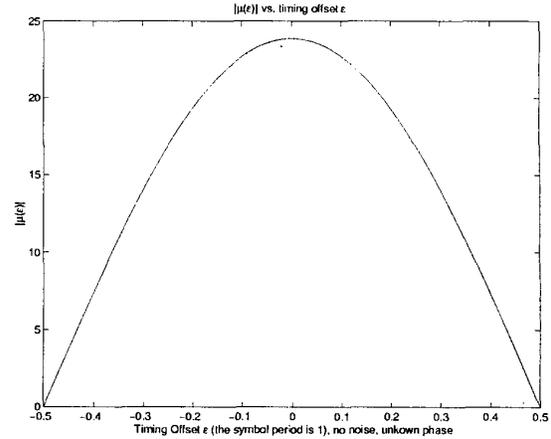

Figure 2: Correlation Magnitude $|\mu(\varepsilon)|$ vs. Timing Offset ε

where $|a_n|^2 = 1$ ($n = 0, \cdots, N - 1$). Furthermore by letting $t = \varepsilon T$ and using Taylor series approximations for sine and cosine functions and after some simplification, we arrive at

$$|\mu(t)| \approx N E_s \left(1 - \frac{\pi^2 t^2}{6T^2} \right) \qquad (9)$$

Figure 2 shows the result of numerical evaluation of $|\mu(\varepsilon)|$ which follows a quadratic form. From eq. (9) we can use a second order polynomial to approximate the relationship between sampling time and the magnitude of correlation $|\mu(t)|$ given that these sampling points are close enough to the ideal sampling point (i.e. t is close enough to 0). Using a general form of the second order polynomial

$$|\mu(t)| = b_2 t^2 + b_1 t + b_0 \qquad (10)$$

suggests that a joint phase and timing estimator can be derived based on three adjacent samples of $|\mu(t)|$. These samples are the closest ones to the ideal sampling point as shown in Figure 3. In order to meet the condition that t is close enough to 0, two
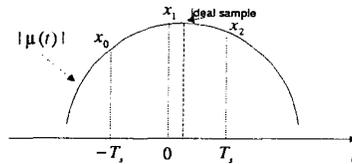

Figure 3: Three Sampling Points Model

measures are adopted: one is that the sampling rate L (samples per symbol) is large enough (simulation shows that $L = 4$ can achieve good performance); second is locating the largest available magnitude x_1 through peak search. Let us define the sampling time of x_1 as nominal 0 on time axis. Therefore the

sampling times of x_0 and x_2 are $-T_s$ and T_s, respectively. A *LaGrange* interpolating polynomial can be adopted based on the values of x_k $(k = 0, 1, 2)$:

$$|\mu(t)| = \sum_{k=0}^{2} x_k \prod_{i=0, i \neq k}^{2} \frac{t - t_i}{t_k - t_i} \qquad (11)$$

$$= b_2 t^2 + b_1 t + b_0$$

where

$$b_2 = \sum_{n=0}^{2} \frac{x_n}{\prod_{l=0, l \neq n}^{2} (t_n - t_l)} \qquad (12)$$

$$b_1 = -\sum_{n=0}^{2} \frac{x_n \sum_{l=0, l \neq n}^{2} t_l}{\prod_{l=0, l \neq n}^{2} (t_n - t_l)} \qquad (13)$$

$$b_0 = \sum_{n=0}^{2} \frac{x_n \prod_{l=0, l \neq n}^{2} t_l}{\prod_{l=0, l \neq n}^{2} (t_n - t_l)} \qquad (14)$$

Using the fact that $t_0 = -T_s$, $t_1 = 0$, $t_2 = T_s$, we can get

$$b_2 = \frac{1}{T_s^2} \left(\frac{x_0}{2} - x_1 + \frac{x_2}{2} \right)$$

$$b_1 = \frac{1}{T_s} \left(\frac{x_2}{2} - \frac{x_0}{2} \right)$$

$$b_0 = x_1$$

The ML timing offset estimator (5) is the $\hat{\varepsilon}$ which maximizes $|\mu(\varepsilon)|$. It is easy to compute the sampling time of the peak of $|\mu(t)|$ from a second order polynomial, i.e.

$$t_{peak} = -\frac{b_1}{2b_2} = \frac{(x_0 - x_2)T_s}{2x_0 - 4x_1 + 2x_2} \qquad (15)$$

therefore, the ML estimate of ε is

$$\hat{\varepsilon} = -\frac{t_{peak}}{T} = \frac{x_2 - x_0}{L(2x_0 - 4x_1 + 2x_2)} \qquad (16)$$

The phase estimator is shown in eq. (6). Interpolation techniques can be applied to correct the timing offset before phase estimation. This however, introduces an additional delay in the demodulation process. Simulations show that using the time for the non-ideal sample of x_1 is sufficient for meeting the CRLB (sampling time of x_1 is t_1). This leads to

$$\hat{\theta} = \arg [\mu(t_1)] \qquad (17)$$

In order to locate the largest available value x_1 easily, a highly correlated data pattern $\underline{a}$ is selected. [2] discusses this problem in depth. Here unique word (UW) and alternating (one zero) data patterns are investigated.

The same algorithms can be applied to OQPSK modulation with minor modifications. $\mu(\varepsilon)$ is slightly modified from eq. (4) as:

$$\mu(\varepsilon) = \sum_{n=0}^{N-1} [a_{n1}^* z(nT + \varepsilon T) + a_{n2}^* z(nT + T/2 + \varepsilon T)] \qquad (18)$$
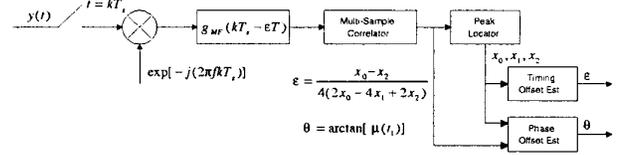

Figure 4: Joint Carrier Phase and Timing Offsets Estimator

where

$$a_{n1} = a_{In} + j \sum_{k=0}^{N-1} a_{Qk} r((n - k - 1/2)T)$$

$$a_{n2} = \sum_{k=0}^{N-1} a_{Ik} r((n - k + 1/2)T) + j a_{Qn}$$

a_{n1} and a_{n2} are defined to combine the effect of inter-channel and inter-symbol interferences. The above however requires more computational power since multipliers are needed instead of just adders for the QPSK case. We can get a simplified version by letting $a_{n1} = a_{In}$ and $a_{n2} = j a_{Qn}$.

Computer simulations show that the performance degradation is small and we can conserve hardware and make the implementation compatible with QPSK. After redefining $\mu(\varepsilon)$, we just need to follow the same procedure derived for QPSK for estimating timing and phase offsets.

3. VLSI IMPLEMENTATION

The hardware block diagram for the estimator is shown in Figure 4. The multi-sample correlator generates outputs at a higher rate than one sample per symbol. Let us define the following complex correlation computation:

$$\mu(\varepsilon) = \sum_{n=0}^{N-1} (a_{In} - j a_{Qn})(z_I(n) + j z_Q(n))$$

$$= \sum_{n=0}^{N-1} (a_{In} z_I(n) + a_{Qn} z_Q(n) + j(a_{In} z_Q(n) - a_{Qn} z_I(n)))$$

$$= C_{II} + C_{QQ} + j(C_{IQ} - C_{QI}) \qquad (19)$$

A systolic [4] VLSI implementation of the correlator is shown in Figure 5 for both QPSK and OQPSK cases, where x_{ij} denotes the ith symbol $(i = 0, \cdots, N - 1)$, jth sample $(j = 0, \cdots, 3)$ of the output from the matched shaping filter. In QPSK/OQPSK case, $a_{Ij} = \pm 1$, $a_{Qj} = \pm 1$, only adders are necessary therefore the computational complexity is relatively small especially when using the correlator as soft-decision UW detector. Through peak search module, we can locate x_0, x_1 and x_2. An *Arctan* Lookup table (LUT) is used when estimating the phase offset.
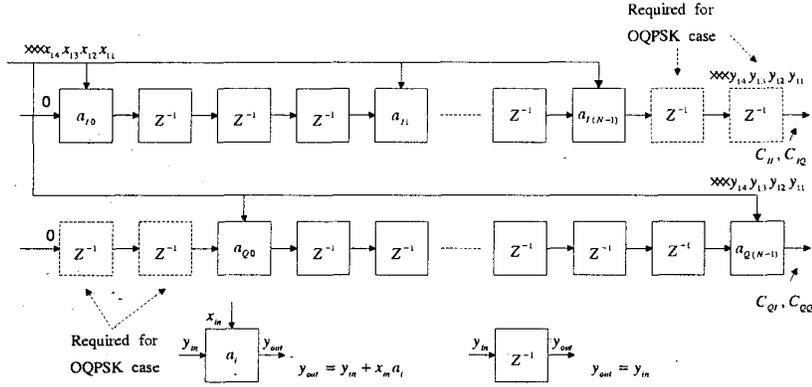
Figure 5: Multi-Sample Correlator for QPSK/OQPSK

4. PERFORMANCE BOUNDS AND SIMULATION RESULTS

The performance lower bound for unbiased ML estimation is the Cramer-Rao lower bound (CRLB). We first address the CRLB for the QPSK case analytically. Then the performance of QPSK and OQPSK is shown through simulations. The $CRLB_{DA}$ for phase estimation is given by [1] as follows:

$$E[(\theta - \hat{\theta})^2] \geq \left\{ \frac{2E_s}{N_0} N \right\}^{-1} \quad (20)$$

Moeneclaey proposed the CRLB for i.i.d. random data pattern (i.e., no information about $\underline{a}$ available) in [3]. The bound for the case where the sampling rate $1/T_s \geq 2B$ (B is the bandwidth of $r(t)$) and N large enough is given by

$$E[(\tau - \hat{\tau})^2] \geq T^2 \left\{ \frac{2E_s}{N_0} N \int 4\pi^2 f^2 \mathcal{R}(f) df \right\}^{-1} \quad (21)$$

with $\mathcal{R}(f)$ the Fourier transform of $r(t)$. Jiang has proposed the following expression for $CRLB_{DA}$ in [2]:

$$\left\{ \frac{2E_s}{N_0 NT} \left[\sum_{k=-K/2}^{K/2-1} \left(\frac{2\pi k}{N} \right)^2 \mathcal{R} \left(\frac{k}{NT} \right) |A[k]|^2 \right] \right\}^{-1} \quad (22)$$

where $A[k]$ is the kth element of N-point discrete Fourier transform (DFT) of $\underline{a}$, i.e. $A[k] = \sum_{n=0}^{N-1} a_n e^{-j(2\pi nk/N)}$. According to eq. (22), $CRLB_{DA}$ has different values for different data patterns. Two data patterns have been investigated: alternating one-zero pattern (i.e. $a_i = (-1)^i \sqrt{2}/2(1+j)$), and a unique word pattern. A 48-symbol UW was selected. According to eq. (22) for the alternating one-zero data pattern

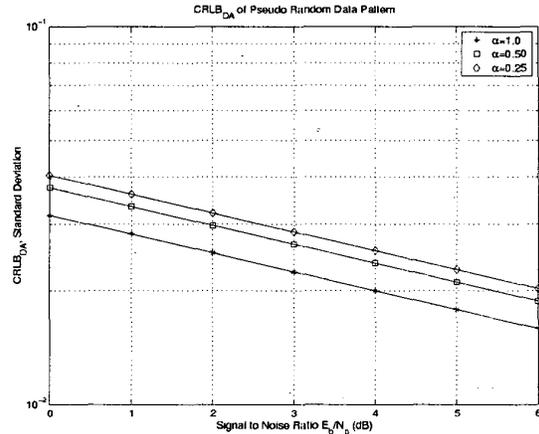$$CRLB_{DA}|_{10} = \left\{ 2\pi^2 \frac{E_s}{N_0} N \right\}^{-1} \quad (23)$$

Figure 6: The $CRLB_{DA}$ for Timing Estimation with UW Pattern

and thus the performance is independent of rolloff factor α given that $\alpha > 0$. For the UW pattern, the timing estimation $CRLB_{DA}$ is closely related to the rolloff factor. It follows from eq. (22) that the larger the rolloff factor, the smaller $CRLB_{DA}$. Figure 6 shows eq. (22) plotted as a function of SNR for three different values of rolloff factor.

The parameters for the computer simulations for QPSK and OQPSK signaling were $N = 48$ and $L = 4$ in an AWGN channel. Figure 7 shows the saw tooth characteristics of eq. (16) under no noise conditions with random phase. From simulations we can see that (16) is an unbiased estimate of ε. Peak search (i.e. locating x_1) resolves the $m/4$ ($m = \pm 1, \pm 2$) ambiguity.

Different rolloff factors for the raised cosine shaping function were also tested. Simulation shows that the root mean squared (RMS) timing estimation error of QPSK meets the $CRLB_{DA}$ for all αs and data patterns. Simulations also support
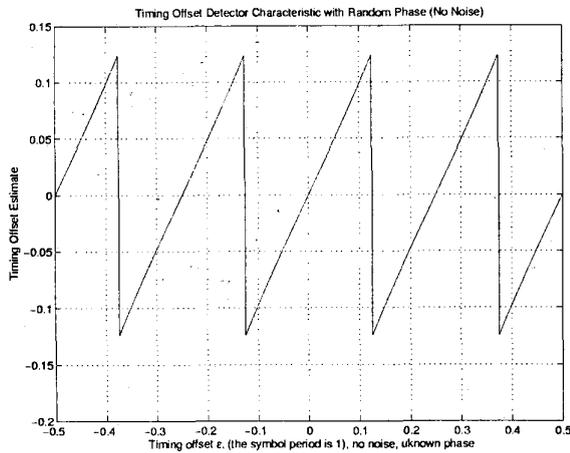
745

Figure 7: Timing Offset Estimate $\hat{\varepsilon}$ vs. Timing Offset ε
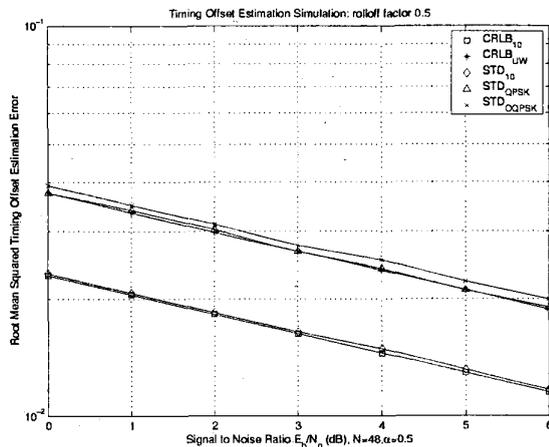

Figure 8: Timing Offset Estimation Performance of QPSK/OQPSK (one zero pattern vs. UW pattern, $\alpha = 0.5$)

that for the one-zero pattern the RMS timing error is independent of α, while for the UW pattern it decreases as α increases. This is in agreement with the evaluation of the $CRLB_{DA}$. For OQPSK case the timing estimation performance degrades slightly compared with QPSK due to the crosstalk between the in-phase and the quadrature channels in the presence of timing and phase offsets. Figure 8 shows the timing offset estimation performance with $\alpha = 0.5$, where one-zero pattern of QPSK and UW pattern of QPSK/OQPSK are illustrated. Figure 9 shows the phase estimation performance. The RMS phase estimation error meets the $CRLB_{DA}$ for phase estimation in QPSK case while it degrades slightly in OQPSK case.
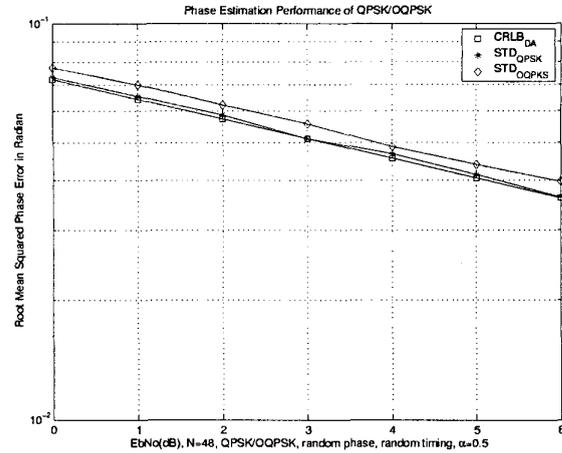

Figure 9: Phase Offset Estimation Performance of QPSK/OQPSK (UW pattern, $\alpha = 0.5$)

5. CONCLUSION

In this paper an ML joint phase and timing offsets estimator for QPSK/OQPSK burst modems along with a systolic VLSI implementation has been presented. The performance of timing recovery meets the CRLB for the DA case at low SNR, therefore it verifies the correctness of this $CRLB_{DA}$ [2]. The joint estimator is relatively simple to realize.

6. REFERENCES

[1] H. Meyr, M. Moeneclaey, S. Fechtel, *Digital Communication Receivers, Synchronization, Channel Estimation, and Signal Processing*, New York: Wiley, 1998.

[2] Yimin Jiang, John S. Baras *"Maximum Likelihood Estimation of Timing Offset: A Frequency Domain Approach"*, to be published.

[3] C. Georahiades, M. Moeneclaey, "Sequence Estimation and Synchronization from Nonsynchronized Samples", *IEEE Trans. Inform. Theory*, vol. IT-37, pp. 1649-1657, Nov. 1991.

[4] H. T. Kung, "Why Systolic Architecture", *IEEE Computer*, vol. 15, no. 1, pp. 37-46 Jan. 1982.